From fractional solitons to Majorana fermions in a paradigmatic model of topological superconductivity

N. Traverso Ziani,[1,2,*] C. Fleckenstein,[3] L. Vigliotti,[1] B. Trauzettel,[3,4] and M. Sassetti[1,2]

[1]*Dipartimento di Fisica, Università di Genova, 16146 Genova, Italy*

[2]*CNR spin, Via Dodecaneso 33, 16146 Genova, Italy*

[3]*Institute of Theoretical Physics and Astrophysics, University of Würzburg, 97074 Würzburg, Germany*

[4]*Würzburg-Dresden Cluster of Excellence ct.qmat, Germany*

(Received 10 February 2020; revised manuscript received 14 March 2020; accepted 20 April 2020; published 11 May 2020)

Majorana bound states are interesting candidates for applications in topological quantum computation. Low-energy models allowing one to grasp their properties are hence conceptually important. The usual scenario in these models is that two relevant gapped phases, separated by a gapless point, exist. In one of the phases, topological boundary states are absent, while the other one supports Majorana bound states. We show that a customary model violates this paradigm. The phase that should not host Majorana fermions supports a fractional soliton exponentially localized at only one end. By varying the parameters of the model, we describe analytically the transition between the fractional soliton and two Majorana fermions. Moreover, we provide a possible physical implementation of the model. We further characterize the symmetry of the superconducting pairing, showing that the odd-frequency component is intimately related to the spatial profile of the Majorana wave functions.

DOI: 10.1103/PhysRevB.101.195303

I. INTRODUCTION

The search for platforms enabling the implementation of operations based on Majorana bound states is a fascinating area in condensed matter physics [1–5]. Such devices represent a substantial step forward for topological quantum computation [6,7]. As of now, the most promising candidates as hosts for Majorana bound states appear to be spin-orbit coupled quantum wires [3–5], planar Josephson junctions [8,9], topological insulators [10,11], and ferromagnetic chains on superconductors [12]. The experimental tools commonly used to substantiate the formation of Majorana bound states in those systems are transport measurements and tunneling spectroscopy. A downside of such detection methods is that it is not easy to discriminate between topological Majorana bound states and trivial Andreev bound states [13–17], disorder [18,19], or distracting effects in Josephson junctions [20–23]. More refined experimental schemes, involving for instance the study of nonlocal conductance [24] and current noise [25], have hence been suggested to better characterize the presence of Majorana fermions. As the complexity of the properties to be inspected increases, the adoption of low-energy models becomes more important to capture the essential physics.

A common trait of most low-energy models for Majorana bound states is that they resemble the Jackiw-Rebbi model [26] in particle-hole space [1]. The Majorana bound states are then located at mass kinks of the model. A competing topological bound state is naturally present in such models. When a spin (or chirality) index is also present, fractional solitons [27–30] can emerge. These topological boundary states carry stable fractional charge [31] and have been predicted to appear in heterostructures based on topological insulators and ferromagnetic insulators [27,28] or quantum point contacts [30]. In lattice models, they arise in Su-Schrieffer-Heeger (SSH) -like systems [32]. They are fundamentally interesting and have been proven to lead to phenomena that can be potentially useful in spintronics [27]. However, they have never been detected in a solid state setup.

Previously, the competition between phases hosting Tamm-Shockley [33] states and Majorana fermions have been predicted in models based on spin-orbit coupled quantum wires [29]. In that case, the appearance of zero modes when a single termination is imposed, has been analyzed.

In this work, we describe a simple superconducting system undergoing a transition between a state characterized by the presence of a single fractional soliton to a state characterized by two Majorana bound states. Our model generalizes the basic idea of a competition of these bound states originally proposed in Ref. [29]. The model is fully solvable with periodic and open boundary conditions at the two ends. When periodic boundary conditions are imposed, a quantum phase transition between gapped phases is present. Unexpectedly, when open boundaries are considered, we show that a zero-energy solution is *always* present. In one phase, the solution is localized at one end of the structure, and in the other phase, it is located at both ends. The first case, being adiabatically connected to $\Delta = 0$, where $\Delta = 0$ is the superconducting pairing, corresponds to a single fractional soliton, the second to two Majorana zero modes. In order to better understand

*traversoziani@fisica.unige.it

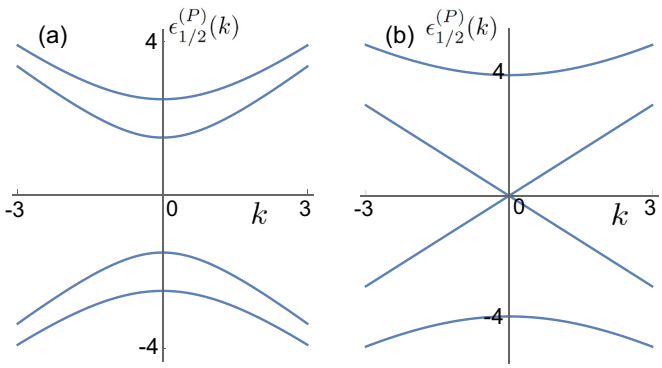

FIG. 1. (a) The dispersion $\epsilon^{(P)}_{1/2}(k)$ in units of v_F/L, as a function of k, in units $1/L$, for $\Delta = 2v_F/L$ and $B = 0.5v_F/L$. (b) The dispersion $\epsilon^{(P)}_{1/2}(k)$ in units of v_F/L as a function of k in units $1/L$, for $\Delta = 2v_F/L$ and $B = 2v_F/L$.

the result, we map our model onto the model describing a heterostructure based on the helical edge states of a two-dimensional topological insulator proximitized by an s-wave superconductor [34–54]. This mapping allows us to fully understand the properties of the original model in terms of competing masses. If we investigate the Majorana phase in more detail, we are able to show a deep connection between Majorana wave function, tunneling density of states, and the odd-frequency component of the anomalous Green's function.

The paper is organized as follows. In Sec. II, we present the model. In Sec. III, we discuss the crossover between the Jackiw-Rebbi soliton and the Majorana fermions. In Sec. IV, we present a possible experimental realization of our findings. In Sec. V, we discuss the pairing amplitude in the Majorana phase. Finally, in Sec. VI, we draw our conclusions.

II. MODEL

The Bogoliubov–de Gennes (BdG) Hamiltonian of the model, on the segment of length L, that we study is ($\hbar = 1$)

$$H = \frac{1}{2}\int_0^L \Psi^\dagger(x)\mathcal{H}(x)\Psi(x)dx, \tag{1}$$

where $\Psi^\dagger(x)=(\psi_R^\dagger(x), \psi_L^\dagger(x), \psi_L(x), -\psi_R(x))$, with $\psi_{R/L}(x)$ Fermi operators, and the Hamiltonian density

$$\mathcal{H}(x) = -iv_F\partial_x\tau_z\otimes\sigma_z - B\tau_0\otimes\sigma_y + \Delta\tau_y\otimes\sigma_0. \tag{2}$$

In Eq. (2), v_F is the Fermi velocity, and B and Δ are real and positive competing masses. Moreover, τ_i/σ_i are Pauli matrices acting, respectively, on particle-hole and R/L space. Importantly, this Hamiltonian emerges, for instance, as a linearized model of a spinless topological superconductor (see Appendix A) at large chemical potential. Imposing periodic boundary conditions on the wave functions, it is easy to obtain the spectrum of the Hamiltonian. It is given by the four excitation energy bands $\epsilon^{(P)}_{1/2}(k) = \pm\sqrt{v_F^2k^2 + \Delta^2 + B^2 \pm 2\Delta B}$, where $k = 2\pi n/L$, with n integer, represents the momentum eigenvalues. The dispersion relation is always gapped except for $B = \Delta$. Moreover, it is even under the exchange of B and Δ [see Figs. 1(a) and 1(b)]. Differently from the case of spin-orbit coupled quantum wires [55,56], the model only has two Fermi points in the absence of masses. Hence, the naive expectation would be that, in the case of open boundary conditions, there are no boundary states if the term proportional to B dominates the gap, while a pair of Majorana bound states appears in the case of a Δ-dominated gap. We show below that the physics of the model is much richer.

To model open boundary conditions, we make the hypothesis that the model emerges from the linearization of a spinless parabolic dispersion [25,57] with p-wave superconductivity parametrized by Δ, and a resonant external field parametrized by B (see Appendix A). The condition for having a resonant field is that it has a substantial component with wave vector $2k_F$ [56]. We hence decompose the Fermi field as $\psi(x) = e^{ik_Fx}\psi_R(x) + e^{-ik_Fx}\psi_L(x)$. The open boundary conditions can then be written as [57]

$$\psi_L(x) = -\psi_R(-x), \tag{3}$$

$$\psi_R(x + 2L) = \psi_R(x). \tag{4}$$

Note that the fields $\psi_R(x)$ and $\psi_L(x)$ are not independent anymore. Moreover, the periodicity in space has doubled, leading to effective momenta $q = n\pi/L$, with n integer. The minus sign relating $\psi_R(x)$ and $\psi_L(-x)$ in Eq. (3) can be understood by observing that a basis $\{\zeta_n(x)\}_{n>0}$ for square integrable functions in the domain $[0, L]$, with open boundary conditions, is given by the functions $\zeta_n(x) = \sqrt{2}L\sin(\frac{n\pi x}{L}) \propto e^{in\pi x/L} - e^{-in\pi x/L}$. The full Fermi field is built from the wave functions $\zeta_n(x)$. In the linearized scheme, the right-moving Fermi field is then given by the terms proportional to $e^{in\pi x/L}$, while the left-moving field by $e^{-in\pi x/L}$. The Hamiltonian (1) is given by

$$H = \int_{-L}^{L} dx[\mathcal{H}_0 + \mathcal{H}_\Delta + \mathcal{H}_B], \tag{5}$$

with

$$\mathcal{H}_0 = v_F\psi_R^\dagger(x)(-i\partial_x)\psi_R(x), \tag{6}$$

$$\mathcal{H}_B = -iB\,\mathrm{sgn}(x)\psi_R^\dagger(x)\psi_R(-x), \tag{7}$$

$$\mathcal{H}_\Delta = i\frac{\Delta}{2}\mathrm{sgn}(x)[\psi_R^\dagger(x)\psi_R^\dagger(-x) + \psi_R(x)\psi_R(-x)], \tag{8}$$

where $\mathrm{sgn}(\cdot)$ is the sign function. For the mapping from the quadratic dispersion of the common p-wave superconductor shown in the Appendix A to the linearized model to be meaningful, band curvature at the chemical potential must give a negligible contribution to the kinetic energy. This condition holds true for large chemical potential.

III. JACKIW-REBBI SOLITONS VS MAJORANA FERMIONS

Solving the Schrödinger equation for the problem amounts to recasting the Hamiltonian in the form $H = \sum_p \epsilon_p c_p^\dagger c_p$, where p is an index for a complete basis of eigenfunctions, ϵ_p is the corresponding energy, and c_p the Fermi operator. To

do so, we make the ansatz

$$c_p^\dagger = \int_{-L}^{L} dx[\chi_p(x)\psi_R^\dagger(x) + \xi_p(x)\psi_R(x)]. \tag{9}$$

We then obtain the following system of differential equations:

$$\epsilon_p\chi_p(x) = -iv_F\partial_x\chi_p(x) + i[\Delta\xi_p(-x) - B\chi_p(-x)]\mathrm{sgn}(x),$$
$$\epsilon_p\xi_p(x) = -iv_F\partial_x\xi_p(x) + i[\Delta\chi_p(-x) - B\xi_p(-x)]\mathrm{sgn}(x).$$

Despite the nonlocal character of the equations, an analytical solution is possible. The method we employ is based on the decomposition

$$\chi_p(x) = \chi_p^+(x)\Theta(x) + \chi_p^-(-x)\Theta(-x),$$
$$\xi_p(x) = \xi_p^+(x)\Theta(x) + \xi_p^-(-x)\Theta(-x), \tag{10}$$

where $\Theta(\cdot)$ is the Heaviside step function.

The additional conditions to be satisfied are $\chi_p^+(0) = \chi_p^-(0)$, $\xi_p^+(0) = \xi_p^-(0)$, $\chi_p^+(L) = \chi_p^-(L)$, and $\xi_p^+(L) = \xi_p^-(L)$. Solutions are found for energies $\epsilon \geqslant |\Delta - B|$ and $\epsilon = 0$. The energy levels in the part of the spectrum for which $\epsilon \geqslant |\Delta - B|$ become dense in the $L \to \infty$ limit. The zero-energy eigenfunction, henceforth labeled by a subscript 0, represents an isolated solution. We find for the zero-energy state

$$\chi_0^+(x) = \chi_0^-(x) = A_0 e^{(\Delta-B)x/v_F} + C_0 e^{-(\Delta+B)x/v_F}, \tag{11}$$

$$\xi_0^+(x) = \xi_0^-(x) = A_0 e^{(\Delta-B)x/v_F} - C_0 e^{-(\Delta+B)x/v_F}. \tag{12}$$

Up to a global phase, the coefficients obey

$$A_0^2 = C^2\frac{\Delta - B}{\Delta + B}e^{-2\Delta L/v_F}\frac{\sinh[(\Delta + B)L/v_F]}{\sinh[(\Delta - B)L/v_F]}, \tag{13}$$

$$C_0^2 = \frac{\Delta + B}{4v_F}\frac{1}{1 - e^{-2(\Delta+B)L/v_F}}. \tag{14}$$

There are two intriguing observations about the zero-energy solution. The first one is that it can be found in both of the gapped regions. This is not what is commonly expected in models for Majorana fermions, for instance, in the Kitaev model, where nontrivial boundary states only appear in the topological sector. The second observation is that for $\Delta > B$ the state is localized in the vicinity of $x = 0$ and $x = L$, while for $\Delta < B$ the state is only localized close to $x = 0$. The first case is the usual Majorana bound state scenario, where the fermionic zero mode is decomposed into two Majorana fermions located at the edges of the system. The second case is reminiscent of a Jackiw-Rebbi fermionic state, where the mass has a single kink. Upon varying B and Δ, our model implements the transition of a Jackiw-Rebbi into two Majorana bound states. This crossover is illustrated in Fig. 2. This behavior is surprising. Indeed, it is difficult to predict the presence of end stated in systems with quadratic kinetic energy. In linear theories, on the other hand, it is well known that bound states appear at mass kinks. When a linear system is built from a quadratic model, as in our case, the original boundary conditions may effectively be translated in such mass kinks. Surprising and unpredictable bound states characterizing quadratic systems can hence be intuitively explained by means of linearization. In the next section we fully exploit this principle in the case of our model.

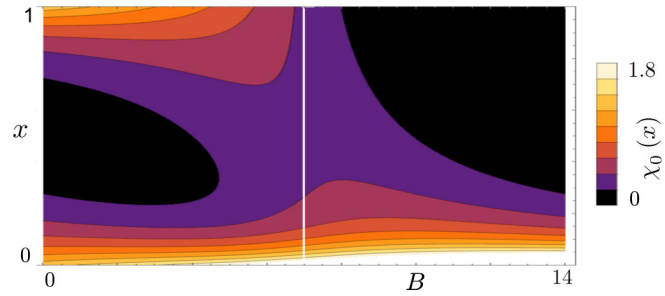

FIG. 2. Contour plot of $\chi_0(x)$, in units $L^{-1/2}$, as a function of B in units v_F/L, and of x, in units L, for $\Delta = 7v_F/L$. The central white line corresponds to the gapless point.

IV. HELICAL EDGE IMPLEMENTATION

The aim of this section is twofold. We present a model based on a quantum spin Hall based heterostructure that both clarifies the result and represents a possible experimental realization of the phenomena we discussed.

To proceed with a physical interpretation, it is useful to enumerate the ingredients leading to the phenomena we have discussed. The presence of four (dependent) Fermi fields, with linear kinetic energy and zero chemical potential is needed. Furthermore, two mass terms acting in different subspaces, relations that implement a dependence between right and left movers and an "unfolding" periodic boundary condition play essential roles. The required number of Fermi fields is provided by a helical edge proximitized by an s-wave superconductor. The boundary conditions are then implemented by two strong magnetic barriers at $x = 0$ and $x = L$. The two masses are provided by the induced superconductivity and by an external magnetic field [58–60]. More specifically, in order to reproduce the correct boundary conditions, the external magnetic field must be positive in the $-\sigma_y$ direction in spin space, the magnetic barrier at $x = 0$ must be positive in the σ_y direction in spin space, while the magnetic barrier at $x = L$ must be parallel to the external magnetic field [42]. Other directions of the magnetization of the barriers would result in twisted boundary conditions instead of Eqs. (3) and (4). For a schematic, see Fig. 3. More specifically, an infinite quantum spin Hall system in the presence of a magnetic gap B_{qsh} and a

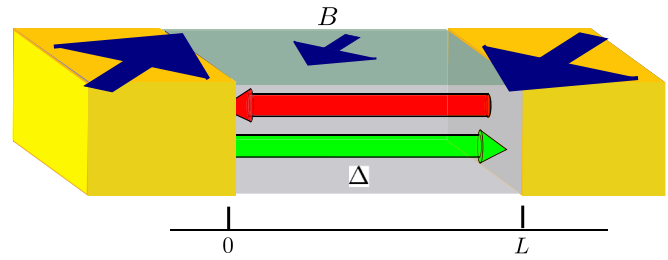

FIG. 3. The quantum spin Hall analogy of the model. The arrows in the central region indicate right- and left-moving particles, the arrows in the side blocks the magnetization of the barriers, and B and Δ the applied magnetic field and the superconducting pairing.

superconducting gap Δ_{qsh} can be modeled by

$$H_{qsh}^{(\infty)} = \int_{-\infty}^{\infty} [\mathcal{H}_{0,qsh}(x) + \mathcal{H}_{B,qsh}(x) + \mathcal{H}_{\Delta,qsh}(x)]dx, \quad (15)$$

where

$$\mathcal{H}_{0,qsh}(x) = \sum_{s=\pm} \psi_{s,qsh}^{\dagger}(x)(-isv_F\partial_x)\psi_{s,qsh}(x), \quad (16)$$

$$\mathcal{H}_{B,qsh}(x) = \sum_{s=\pm} isB_{qsh}\psi_{s,qsh}^{\dagger}(x)\psi_{-s,qsh}(x), \quad (17)$$

$$\mathcal{H}_{\Delta,qsh}(x) = \Delta_{qsh}\psi_{+,qsh}^{\dagger}(x)\psi_{-,qsh}^{\dagger}(x) + \text{H.c.} \quad (18)$$

Here, s represents the spin projection and $\psi_{s,qsh}^{\dagger}(x)$ is the creation operator of a fermionic field for an electron with spin projection s. The Hamiltonian density is identical to the one in Eq. (1), provided that the fermionic fields of the two theories are identified. To proceed with the analogy, boundary conditions need to be implemented. To this aim, strong magnetic barriers are added at $x = 0$ and $x = L$. The corresponding Hamiltonian H_G is

$$H_G = \int_{-\infty}^{\infty} \sum_s \psi_{s,qsh}^{\dagger}(x)\big[\big(M_x^{(0)} - isM_y^{(0)}\big)\delta(x) + \big(M_x^{(L)} - isM_y^{(L)}\big)\delta(x-L)\big]\psi_{s,qsh}(x)dx. \quad (19)$$

In Eq. (19), $M_{x/y}^{(0/L)}$ represents the various components of the magnetization of the barriers. In the limit $\sqrt{M_x^{(0/L)2} + M_y^{(0/L)2}}/v_F \gg 1$, the regions $x < 0$, $0 < x < L$, and $x > L$ become fully separated. The boundary conditions that the fields in the region $0 < x < L$ obey are [42]

$$\psi_{+,qsh}(0) = \left[\frac{-M_y^{(0)} - iM_x^{(0)}}{M_x^{(0)2} + M_y^{(0)2}}\right]\psi_{-,qsh}(0), \quad (20)$$

$$\psi_{+,qsh}(L) = \left[\frac{M_y^{(L)} + iM_x^{(L)}}{M_x^{(L)2} + M_y^{(L)2}}\right]\psi_{-,qsh}(L). \quad (21)$$

To reproduce the open boundary conditions emerging from Eqs. (3) and (4), that is, $\psi_{+,qsh}(0) = -\psi_{-,qsh}(0)$ and $\psi_{+,qsh}(L) = -\psi_{-,qsh}(L)$, we need to set $M_x^{(0)} = M_x^{(L)} = 0$, $M_y^{(0)} > 0$, and $M_y^{(L)} < 0$. Once the boundary conditions are known, it is easy to obtain the solution to the single-particle problem, and hence demonstrate that $\psi_{+,qsh}(x) = -\psi_{-,qsh}(-x)$. Moreover, with this choice of the magnetization direction of the barriers, we have $\psi_{+,qsh}(x) = \psi_{+,qsh}(x + 2L)$. When the magnetization of the barriers is not antiparallel, twisted boundary conditions emerge. The Hamiltonian of the part of the helical edge confined between the magnetic barriers is hence equal to the problem already solved [Eqs. (5)–(8)]. To show this fact, the identifications $\psi_{\pm,qsh}(x) \to \psi_{R/L}(x)$, $\Delta_{qsh} \to \Delta$, and $B_{qsh} \to B$ must be performed. This analogy completely clarifies the obtained results: When the gap is of superconducting type, two Majorana fermions are present at the boundaries. On the other hand, when the gap is of magnetic type, a Jackiw-Rebbi charge is trapped close to $x = 0$ since there the mass (the magnetization of the barrier/the magnetic field) changes sign. The mapping of the model onto a heterostructure based on the edges of a two-dimensional topological insulator not only provides a valuable tool for understanding the transmutation of the Jackiw-Rebbi charge into Majorana fermions. It also provides a possible experimental realization of the model and implies that the standard techniques used to address the transport properties of topological heterostructures can be employed in the case of finite magnetic barriers. Even more importantly, the mapping onto the setup based on the helical system provides a detection scheme for the transition. Indeed, for a large but not infinite magnetic barrier, and in the limit of large L, the linear local differential conductance vanishes in the trivial case, for large L, while it is quantized to $2e^2/h$ in the topological phase [60].

V. $B = 0$ PHASE

In this section, we carefully investigate the $B = 0$ regime. In this case, the Hamiltonian density can be written as a 2×2 differential quadratic operator. One has $H = \int_0^L \Psi^{\dagger}(x)\mathcal{H}(x)\Psi(x)dx$, with $\mathcal{H} = -iv_F\partial_x\tau_z - i\Delta\tau_x$. Correspondingly, the Fermi spinor acquires two components only. As a first step, we state the inverse of Eq. (10), that reads

$$\psi_R(x) = \sum_p [\xi_p^*(x)c_p^{\dagger} + \chi_p(x)c_p]. \quad (22)$$

The explicit form of the functions $\xi_p(x)$ and $\chi_p(x)$ is given in the Appendix. By using Eqs. (3) and (4), we define the Majorana field operators $\gamma_1(x)$ and $\gamma_2(x)$ in the usual way [1]:

$$\gamma_1(x) = i[\Psi^{\dagger}(x) - \Psi(x)], \quad (23)$$

$$\gamma_2(x) = [\Psi^{\dagger}(x) + \Psi(x)]. \quad (24)$$

The zero-energy contributions $\gamma_1^{(0)}, \gamma_2^{(0)}$ to the Majorana fields, that is, the Majorana zero modes, then read

$$\gamma_1^{(0)}(x) = \frac{2\sin(k_F x)\sqrt{\Delta/v_F}}{\sqrt{1 - e^{-2\Delta L/v_F}}} e^{-\Delta(L-x)/v_F}(c_0^{\dagger} + c_0), \quad (25)$$

$$\gamma_2^{(0)}(x) = \frac{-2i\sin(k_F x)\sqrt{\Delta/v_F}}{\sqrt{1 - e^{-2\Delta L/v_F}}} e^{-\Delta x/v_F}(c_0^{\dagger} - c_0). \quad (26)$$

We recover the expected results, namely, that one Majorana zero mode is located close to $x = 0$ ($\gamma_2^{(0)}$) and one close to $x = L$ ($\gamma_1^{(0)}$). Moreover, $2k_F$ oscillations appear in accordance with the fact that we have imposed a sharp confinement potential [61]. Note that, within the model, the two Majorana modes do not hybridize.

Another feature of the model is that the Green's functions can be calculated analytically. This allows us to show explicitly the intimate connection between the spatial extension of the Majorana zero modes given in Eqs. (18) and (19) and the odd-frequency component of the superconducting pairing that characterizes the topological superconductor.

We define the retarded Green's function $G_{ij}^R(x, x', \omega)$ as [62]

$$G_{ij}^R(x, x', \omega) = \int_{-\infty}^{\infty} e^{i\omega(t+i0^+)} G_{ij}^R(x, x', t)dt, \quad (27)$$

with

$$G_{ij}^R(x, x', t) = -i\theta(t)\langle\{\Psi_i(x, t), \Psi_j^{\dagger}(x', 0)\}\rangle, \quad (28)$$

where $\Psi_i(x, t)$ $(i = 1, 2)$ are the components of the Nambu spinor in the Heisenberg picture. The average is performed

on the ground state and the braces indicate the anticommutator. The advanced Green's function $G^A_{ij}(x,x',\omega)$ is given by $G^{A*}_{ij}(x,x',\omega) = G^R_{ji}(x',x,\omega)$. Due to particle-hole symmetry of the BdG Hamiltonian, the components of the Green's functions are not independent, but satisfy

$$G^R_{ij}(x,x',\omega) = -\sigma_x^{il} G^{R*}_{lm}(x,x',-\omega)\sigma_x^{mj}. \tag{29}$$

Moreover, focusing on the anomalous part of the Green's function, that is, on the off-diagonal parts, we have $G^A_{21}(x',x,\omega) = -G^R_{21}(x,x',-\omega)$. The function $\mathcal{F}(x,x',\omega) = G^R_{21}(x,x',\omega) + G^A_{21}(x,x',\omega)$ hence satisfies

$$\mathcal{F}(x,x',\omega) + \mathcal{F}(x',x,-\omega) = 0. \tag{30}$$

Consequently,

$$\mathcal{F}_+(x,x',\omega) = \frac{\mathcal{F}(x,x',\omega) + \mathcal{F}(x',x,\omega)}{2} \tag{31}$$

is odd in ω and characterizes the odd-frequency pairing. Odd-frequency pairing can be expected to be related to the Majorana wave function, because a Majorana zero mode is an intrinsically odd-frequency object [49]. In our model, we find, for $\omega < \Delta$,

$$\mathcal{F}_+(x,x,\omega) = \frac{4\pi P\left(\frac{1}{\omega}\right)}{\sinh[L\sqrt{\Delta^2-\omega^2}]}\zeta(x), \tag{32}$$

where $P(\cdot)$ is the Cauchy principal value and

$$\zeta(x) = \sin^2(k_F x)\sinh[(L-2x)\sqrt{\Delta^2-\omega^2}/v_F]. \tag{33}$$

For $(L-2x)/L \simeq 1$ $[(L-2x)/L \simeq -1]$, that is, close to the edges of the system, the odd-frequency pairing resembles the modulus square of the spatial extension of $\gamma_2^{(0)}$ ($\gamma_1^{(0)}$). This intriguing dependence has recently been analyzed in different setups [35,39], including the Kitaev chain [63–67].

In the remainder, we address the question whether the Majorana wave function and the odd-frequency pairing can be measured. The answer, as for other models of (topological) superconductivity [34,39,65,66], is related to the diagonal part $G^R_{11}(x,x,\omega)$ of the Green's function. As an example of a measurable quantity that can be extracted from the retarded Green's function, we in fact analyze the tunneling density of states $\rho(x,\omega) = -\mathrm{Im}G^R_{11}(x,x,\omega)/\pi$, which is associated with the tunneling from a metallic tip at position x above the topological superconductor [62]. The explicit result for the Green's function, for $\omega < \Delta$, reads (see also Ref. [68])

$$\begin{aligned} G^R_{11}(x,x,\omega) = {} & \frac{\omega}{\sqrt{\Delta^2-\omega^2}}[F(\omega,x) - F(\omega,0)] \\ & + \frac{2}{\omega}\sqrt{\Delta^2-\omega^2}F(\omega,x)\sin^2(k_F x) \\ & - \sin(2k_F x)\frac{\sinh[(L-2x)\sqrt{\Delta^2-\omega^2}/v_F]}{\sinh(L\sqrt{\Delta^2-\omega^2}/v_F)}, \end{aligned} \tag{34}$$

with

$$F(\omega,x) = \frac{\cosh[\sqrt{\Delta^2-\omega^2}(L-2x)/v_F]}{\sinh(L\sqrt{\Delta^2-\omega^2}/v_F)}. \tag{35}$$

The full Green's function does not show a pronounced similarity with the Majorana wave function and the odd-frequency pairing. However, we find that

$$\rho(x,\omega) = 2\Delta\delta(\omega)\sin^2(k_F x)\frac{\cosh[\Delta(L-2x)/v_F]}{\sinh(\Delta L/v_F)}. \tag{36}$$

The tunneling density of states has hence the same short-wavelength components as the odd-frequency pairing, that is, $\sin^2(k_F x)$, while its envelope function is given by the derivative of the function enveloping the odd-frequency pairing.

The tunneling density of states in the Jackiw-Rebbi case would be much larger at one end than at the other one. The tunneling from a metallic tip hence discriminates the Jackiw-Rebbi from the Majorana case.

VI. CONCLUSIONS

In conclusion, we have proposed and analytically solved a quantum wire model that is characterized by a transition between a state hosting a single Jackiw-Rebbi soliton and a state with two unpaired Majorana fermions. We have explained the results on the basis of a hybrid system involving topological edge channels, superconductivity, and magnetic gaps. Such a setup also allows for the detection of the transition between the phase hosting the fractional soliton and the Majorana phase, by means of a local conductance experiment. We have then characterized the Majorana phase of the system on the basis of the correlation functions. We have shown that the odd-frequency component of the pairing closely follows the spatial extension of the Majorana bound states. After computing the retarded Green's function, we have proposed that the tunneling density of states indeed provides information about the Majorana wave function and the odd-frequency pairing.

ACKNOWLEDGMENTS

We thank Felix Keidel for useful discussions. This work was supported by the DFG (SPP1666, SFB1170 "ToCoTronics"), the Würzburg-Dresden Cluster of Excellence ct.qmat, EXC2147, project-id 39085490, the Elitenetzwerk Bayern Graduate School on "Topological insulators," and the Studienstiftung des Deutschen Volkes.

APPENDIX A: LINEARIZATION OF THE FINITE *p*-WAVE SUPERCONDUCTOR

The starting point is a spinless p-wave superconductor, with Hamiltonian ($\hbar = 1$)

$$\begin{aligned} H_2 = \int_0^L dx \Big\{ & \psi^\dagger(x)\left(-\frac{\partial_x^2}{2m^*} - \mu + B_2\sin(2k_F x)\right)\psi(x) \\ & + [\Delta_2\psi^\dagger(x)\partial_x\psi^\dagger(x) + \mathrm{H.c.}]\Big\}. \end{aligned} \tag{A1}$$

In Eq. (1), ψ is the Fermi operator, μ the chemical potential, $k_F = \sqrt{2\mu m^*}$ the Fermi momentum, m^* the effective mass, Δ_2 the p-wave pairing potential, and B_2 a competing mass. The term proportional to B_2 can emerge, for example, due to the interplay with phonons [69,70], or can be artificially engineered by external gates capacitively coupled to the system [33,71,72]. For large enough chemical potential, we can safely perform the linearization of the theory around

the Fermi points, identifying $v_F = \sqrt{2\mu/m^*}$ as Fermi velocity. With periodic boundary conditions, the diagonalization is straightforward. With open boundary conditions for the fermionic operator $\psi(0) = \psi(L) = 0$, the procedure is more cumbersome but similar to Ref. [57]. One has

$$\psi(x) = e^{ik_F x}\psi_R(x) + e^{-ik_F x}\psi_L(x), \tag{A2}$$

with $\psi_R(x)$ and $\psi_L(x)$ obeying the boundary conditions reported in Eqs. (4) and (5). Explicitly,

$$\psi_R(x) = \frac{-i}{\sqrt{2L}} \sum_{n=-\infty}^{\infty} e^{in\pi x/L} c_{(n+L)k_F/\pi}, \tag{A3}$$

with c_p the fermionic operator annihilating an electron with wave function $\zeta(x) = \sqrt{2/L}\,\sin(p\pi x/L)$. By neglecting fast oscillating terms, in the limit $Lk_F/\pi \gg 1$, and upon renormalization of the parameters ($B = B_2/2$, $\Delta = \Delta_2 k_F$), the Hamiltonian in Eq. (6) is recovered. One comment is in order: Since $\Delta = k_F\Delta_2$ and the linearization is only valid for large k_F, in view of the fact that the gap in the spinless topological superconductor diverges as the chemical potential tends to infinity, the linear model only describes the properties of the original quadratic model in the limit of large gap. This means that little or no hybridization of the Majorana modes is expected.

APPENDIX B: EIGENFUNCTIONS

We provide the explicit expression for the eigenfunctions in Eq. (11) that correspond to nonzero energy, in the case $B = 0$. From the eigenfunctions, the Green's functions are calculated analytically.

We find

$$\chi_q^{(+)} = A_+^{(q)} e^{i\pi q\, x/L} + B_+^{(q)} e^{-i\pi qx/L}, \tag{B1}$$

$$\chi_q^{(-)} = A_-^{(q)} e^{i\pi qx/L} + B_-^{(q)} e^{-i\pi qx/L}, \tag{B2}$$

$$\xi_q^{(+)} = C_+^{(q)} e^{i\pi qx/L} + D_+^{(q)} e^{-i\pi qx/L}, \tag{B3}$$

$$\xi_q^{(-)} = C_-^{(q)} e^{i\pi qx/L} + D_-^{(q)} e^{-i\pi qx/L}, \tag{B4}$$

where q is a positive integer. The corresponding excitation energies are $\epsilon_q = \sqrt{v_F^2\pi^2 q^2/L^2 + \Delta^2}$. The solutions for negative energy $\epsilon_q = -\sqrt{v_F^2 q^2 + \Delta^2}$ are the complex conjugate of the negative of the solutions with positive eigenvalue. This fact can be directly inferred from the symmetries of the Hamiltonian in Eq. (1), with $B = 0$.

For q positive and even, we obtain the coefficients

$$A_+^{(q)} = \frac{\epsilon_q + v_F\pi q/L}{\sqrt{8L\epsilon_q}}, \tag{B5}$$

$$A_-^{(q)} = -\frac{\epsilon_q - v_F\pi q/L}{\epsilon_q + v_F\pi q/L} A_+, \tag{B6}$$

$$B_+^{(q)} = A_-^{(q)}, \tag{B7}$$

$$B_-^{(q)} = A_+^{(q)}, \tag{B8}$$

$$C_+^{(q)} = C_-^{(q)}, \tag{B9}$$

$$C_-^{(q)} = -\frac{i\Delta}{\sqrt{8L\epsilon_q}}, \tag{B10}$$

$$D_+^{(q)} = -C_+^{(q)}, \tag{B11}$$

$$D_-^{(q)} = -C_-^{(q)}. \tag{B12}$$

For q odd, we have to replace $A_\pm^{(q)} \leftrightarrow C_\pm^{(q)}$, $B_\pm^{(q)} \leftrightarrow D_\pm^{(q)}$.

[1] Y. Oreg, G. Refael, and F. von Oppen, Phys. Rev. Lett. **105**, 177002 (2010).

[2] R. M. Lutchyn, J. D. Sau, and S. Das Sarma, Phys. Rev. Lett. **105**, 077001 (2010).

[3] V. Mourik, K. Zuo, S. M. Frolov, S. R. Plissard, E. P. A. M. Bakkers, and L. P. Kouwenhoven, Science **336**, 1003 (2012).

[4] M. T. Deng, S. Vaitiekenas, E. B. Hansen, J. Danon, M. Leijnse, K. Flensberg, J. Nygard, P. Krogstrup, and C. M. Marcus, Science **354**, 1557 (2016).

[5] S. M. Albrecht, A. P. Higginbotham, M. Madsen, F. Kuemmeth, T. S. Jespersen, J. Nygrd, P. Krogstrup, and C. M. Marcus, Nature (London) **531**, 206 (2016).

[6] A. Y. Kitaev, Phys. Usp. **44**, 131 (2001).

[7] C. Nayak, S. H. Simon, A. Stern, M. Freedman, and S. Das Sarma, Rev. Mod. Phys. **80**, 1083 (2008).

[8] A. Fornieri, A. M. Whiticar, F. Setiawan, E. Portolés Marín, A. C. C. Drachmann, A. Keselman, S. Gronin, C. Thomas, T. Wang, R. Kallaher, G. C. Gardner, E. Berg, M. J. Manfra, A. Stern, C. M. Marcus, and F. Nichele, Nature (London) **569**, 89 (2019).

[9] H. Ren, F. Pientka, S. Hart, A. Pierce, M. Kosowsky, L. Lunczer, R. Schlereth, B. Scharf, E. M. Hankiewicz, L. W. Molenkamp, B. I. Halperin, and A. Yacoby, Nature (London) **569**, 93 (2019).

[10] J. Wiedenmann, E. Bocquillon, R. S. Deacon, S. Hartinger, O. Herrmann, T. M. Klapwijk, L. Maier, C. Ames, C. Brüne, C. Gould, A. Oiwa, K. Ishibashi, S. Tarucha, H. Buhmann, and L. W. Molenkamp, Nat. Commun. **7**, 10303 (2016).

[11] C. Fleckenstein, N. Traverso Ziani, A. Calzona, M. Sassetti, and B. Trauzettel, arXiv:2001.03475.

[12] S. Nadj-Perge, I. K. Drozdov, J. Li, H. Chen, S. Jeon, J. Seo, A. H. MacDonald, B. A. Bernevig, and A. Yazdani, Science **346**, 602 (2014).

[13] J. Cayao, E. Prada, P. San-Jose, and R. Aguado, Phys. Rev. B **91**, 024514 (2015).

[14] P. San-Jose, J. Cayao, E. Prada, and R. Aguado, Sci. Rep. **6**, 21427 (2016).

[15] C. Fleckenstein, F. Dominguez, N. Traverso Ziani, and B. Trauzettel, Phys. Rev. B **97**, 155425 (2018).

[16] C. Moore, T. D. Stanescu, and S. Tewari, Phys. Rev. B **97**, 165302 (2018).
[17] O. A. Awoga, J. Cayao, and A. M. Black-Schaffer, Phys. Rev. Lett. **123**, 117001 (2019).
[18] D. Bagrets and A. Altland, Phys. Rev. Lett. **109**, 227005 (2012).
[19] J. Liu, A. C. Potter, K. T. Law, and P. A. Lee, Phys. Rev. Lett. **109**, 267002 (2012).
[20] H. J. Kwon, K. Sengupta, and V. M. Yakovenko, Eur. Phys. J. B **37**, 349 (2004).
[21] J. Michelsen, V. S. Shumeiko, and G. Wendin, Phys. Rev. B **77**, 184506 (2008).
[22] A. Zazunov, S. Plugge, and R. Egger, Phys. Rev. Lett. **121**, 207701 (2018).
[23] C. K. Chiu and S. Das Sarma, Phys. Rev. B **99**, 035312 (2019).
[24] E. Prada, R. Aguado, and P. San-Jose, Phys. Rev. B **96**, 085418 (2017).
[25] T. Jonckheere, J. Rech, A. Zazunov, R. Egger, A. L. Yeyati, and T. Martin, Phys. Rev. Lett. **122**, 097003 (2019).
[26] R. Jackiw and C. Rebbi, Phys. Rev. D **13**, 3398 (1976).
[27] X.-L. Qi, T. L. Hughes, and S.-C. Zhang, Nat. Phys. **4**, 273 (2008).
[28] J. I. Väyrynen and T. Ojanen, Phys. Rev. Lett. **107**, 166804 (2011).
[29] J. Klinovaja, P. Stano, and D. Loss, Phys. Rev. Lett. **109**, 236801 (2012).
[30] C. Fleckenstein, N. Traverso Ziani, and B. Trauzettel, Phys. Rev. B **94**, 241406(R) (2016).
[31] S. Kivelson and J. R. Schrieffer, Phys. Rev. B **25**, 6447 (1982).
[32] A. J. Heeger, S. Kivelson, J. R. Schrieffer, and W.-P. Su, Rev. Mod. Phys. **60**, 781 (1988).
[33] S. Gangadharaiah, L. Trifunovic, and D. Loss, Phys. Rev. Lett. **108**, 136803 (2012).
[34] Y. Tanaka, Y. Tanuma, and A. A. Golubov, Phys. Rev. B **76**, 054522 (2007).
[35] Y. Tanaka, A. A. Golubov, S. Kashiwaya, and M. Ueda, Phys. Rev. Lett. **99**, 037005 (2007).
[36] M. Eschrig, T. Löfwander, T. Champel, J. C. Cuevas, J. Kopu, and G. Schön, J. Low Temp. Phys. **147**, 457 (2007).
[37] L. Fu and C. L. Kane, Phys. Rev. Lett. **100**, 096407 (2008).
[38] L. Fu and C. L. Kane, Phys. Rev. B **79**, 161408(R) (2009).
[39] Y. Tanaka, M. Sato, and N. Nagaosa, J. Phys. Soc. Jpn. **81**, 011013 (2012).
[40] A. M. Black-Schaffer and A. V. Balatsky, Phys. Rev. B **86**, 144506 (2012).
[41] Y. Asano and Y. Tanaka, Phys. Rev. B **87**, 104513 (2013).
[42] G. Dolcetto, N. Traverso Ziani, M. Biggio, F. Cavaliere, and M. Sassetti, Phys. Rev. B **87**, 235423 (2013).
[43] G. Dolcetto, N. Traverso Ziani, M. Biggio, F. Cavaliere, and M. Sassetti, Phys. Status Solidi RRL **7**, 1059 (2013).
[44] S. Hart, H. Ren, T. Wagner, P. Leubner, M. Mühlbauer, C. Brüne, H. Buhmann, L. W. Molenkamp, and A. Yacoby, Nat. Phys. **10**, 638 (2014).
[45] F. Crepin, P. Burset, and B. Trauzettel, Phys. Rev. B **92**, 100507(R) (2015).
[46] L. Arrachea and F. von Oppen, Physica E **74**, 596 (2015).
[47] G. Dolcetto, M. Sassetti, and T. L. Schmidt, Riv. Nuovo Cimento **39**, 113 (2016).
[48] F. Keidel, P. Burset, and B. Trauzettel, Phys. Rev. B **97**, 075408 (2018).
[49] F. Dominguez, O. Kashuba, E. Bocquillon, J. Wiedenmann, R. S. Deacon, T. M. Klapwijk, G. Platero, L. W. Molenkamp, B. Trauzettel, and E. M. Hankiewicz, Phys. Rev. B **95**, 195430 (2017).
[50] J. Pico-Cortes, F. Dominguez, and G. Platero, Phys. Rev. B **96**, 125438 (2017).
[51] O. Kashuba, B. Sothmann, P. Burset, and B. Trauzettel, Phys. Rev. B **95**, 174516 (2017).
[52] J. Cayao and A. M. Black-Schaffer, Phys. Rev. B **96**, 155426 (2017).
[53] C. Fleckenstein, N. T. Ziani, and B. Trauzettel, Phys. Rev. B **97**, 134523 (2018).
[54] C. Fleckenstein, N. Traverso Ziani, and B. Trauzettel, Phys. Rev. Lett. **122**, 066801 (2019).
[55] P. Streda and P. Seba, Phys. Rev. Lett. **90**, 256601 (2003).
[56] T. Meng and D. Loss, Phys. Rev. B **88**, 035437 (2013).
[57] M. Fabrizio and A. O. Gogolin, Phys. Rev. B **51**, 17827 (1995).
[58] D. L. Maslov, M. Stone, P. M. Goldbart, and D. Loss, Phys. Rev. B **53**, 1548 (1996).
[59] C. Timm, Phys. Rev. B **86**, 155456 (2012).
[60] C. Fleckenstein, F. Keidel, B. Trauzettel and N. Traverso Ziani, Eur. Phys. J.: Spec. Top. **227**, 1377 (2018).
[61] J. Klinovaja and D. Loss, Phys. Rev. B **86**, 085408 (2012).
[62] H. Bruus and K. Flesberg, *Many-Body Quantum Theory in Condensed Matter* (Physics Oxford University Press, Oxford, 2004).
[63] A. Tsintzis, A. M. Black-Schaffer, and J. Cayao, Phys. Rev. B **100**, 115433 (2019).
[64] S. Tamura, S. Hoshino, and Y. Tanaka, Phys. Rev. B **99**, 184512 (2019).
[65] D. Takagi, S. Tamura, and Y. Tanaka, Phys. Rev. B **101**, 024509 (2020).
[66] D. Kuzmanovski, A. M. Black-Schaffer, and J. Cayao, Phys. Rev. B **101**, 094506 (2020).
[67] J. Cayao, C. Triola, and A. M. Black-Schaffer, Eur. Phys. J.: Spec. Top. **229**, 545 (2020).
[68] A. Zazunov, R. Egger, and A. Levy Yeyati, Phys. Rev. B **94**, 014502 (2016).
[69] H. Fröhlich, Proc. R. Soc. London A **223**, 296 (1954).
[70] R. E. Peierls, *Quantum Theory of Solids* (Clarendon, Oxford, 1955).
[71] J. Klinovaja and D. Loss, Phys. Rev. Lett. **110**, 126402 (2013); D. Rainis, A. Saha, J. Klinovaja, L. Trifunovic, and D. Loss, *ibid.* **112**, 196803 (2014); J. Klinovaja and D. Loss, Phys. Rev. B **92**, 121410(R) (2015);
[72] M. Malard, G. I. Japaridze, and H. Johannesson, Phys. Rev. B **94**, 115128 (2016).